REPORT DOCUMENTATION PAGE

Form Approved
OMB No. 0704-0188

1. REPORT DATE *(DD-MM-YYYY)*	2. REPORT TYPE	3. DATES COVERED *(From - To)*
31/12-2018	Performance/Technical Report (Quarterly)	10/1/2018 – 12/31/2018

4. TITLE AND SUBTITLE
A Hybrid Approach to Composite Damage and Failure Analysis Combining Synergistic Damage Mechanics and Peridynamics

5a. CONTRACT NUMBER

5b. GRANT NUMBER
N00014-16-1-2173

5c. PROGRAM ELEMENT NUMBER

6. AUTHOR(S)
Dr. Ramesh Talreja

5d. PROJECT NUMBER

5e. TASK NUMBER

5f. WORK UNIT NUMBER

7. PERFORMING ORGANIZATION NAME(S) AND ADDRESS(ES)
Texas A&M Engineering Experiment Station (TEES)
400 Harvey Mitchell Parkway, Suite 300
College Station, Texas 77845

8. PERFORMING ORGANIZATION REPORT NUMBER
M1601473 / 505170-00001/2

9. SPONSORING / MONITORING AGENCY NAME(S) AND ADDRESS(ES)
Office of Naval Research
875 N. Randolph Street, Suite 1425
Arlington, VA 22203-1995

10. SPONSOR/MONITOR'S ACRONYM(S)
ONR

11. SPONSOR/MONITOR'S REPORT NUMBER(S)

12. DISTRIBUTION / AVAILABILITY STATEMENT
unlimited

13. SUPPLEMENTARY NOTES

14. ABSTRACT

The work performed in the reporting period has been focused on completion of Tasks 1.2 on ply lavel cracking and 1.3 related to Synergistic Damage Mechanics and Tasks 2.2 and 2.4 related to Peridynamics, as described in the project proposal. The activities related to Tasks 1.2 and 1.3 concern initiation of early failure events in the environment of the disordered fiber distribution and matrix voids under the combined action of axial shear and transverse tension. The activities related to Task 2 cover a peridynamic model for fracture initiation in transverse loading of a fiber reinforced composite.

15. SUBJECT TERMS
Computational micromechanics; Cavitation induced cracking; Peridynamics; Porous media

16. SECURITY CLASSIFICATION OF:			17. LIMITATION OF ABSTRACT	18. NUMBER OF PAGES	19a. NAME OF RESPONSIBLE PERSON
a. REPORT	b. ABSTRACT	c. THIS PAGE			William Nickerson
U	U	U	SAR	5	19b. TELEPHONE NUMBER *(include area code)* 703-696-8485

Quarterly Progress Report, April 1 – June 30, 2018

A Hybrid Approach to Composite Damage and Failure Analysis Combining Synergistic Damage Mechanics and Peridynamics

Award Number N00014-16-1-2173

DOD – NAVY – Office of Naval Research

PI: Ramesh Talreja
Co-PI: Florin Bobaru

Executive Summary

The work performed in the reporting period has been focused on completion of Tasks 1.2 on ply lavel cracking and 1.3 related to Synergistic Damage Mechanics and Tasks 2.2 and 2.4 related to Peridynamics, as described in the project proposal. The activities related to Tasks 1.2 and 1.3 concern initiation of matrix cracks and yielding in the environment of the disordered fiber distribution under axial shear. The activities related to Task 2 cover a peridynamic model for fracture initiation in transverse loading of a fiber bundle composite previously analyzed using the Synergistic Damage Mechanics.

Tasks 1.2 and 1.3 Modeling of RVE based initiation of matrix ply cracks under axial shear

In order to apply axial shear to a RVE, the previous 2-dimensional RVE used for the transverse loading case was expanded to add finite elements in the thickness direction. An example of one RVE realization is shown in Fig. 1. The RVE of 14X14 fibers was subjected to periodic boundary conditions.

The local stress fields were determined under thermal cooldown, $\Delta T = -82^{\circ}C$, which is typical of epoxy based composites, followed by uniaxial or biaxial displacements with an incremental strain increase. The local stress states were analyzed for each constructed realization for 40%, 54% and 60% fiber volume fractions and 0%, 60% and 100% degree of nonuniformity. An ABAQUS subroutine was built to calculate the dilatational and distortional energy densities at every node within the RVE at each applied strain for all combinations of fiber volume fractions and the preselected degree of nonuniformity. The maximum dilatational energy density was determined, provided that the three principal stresses were tensile. The principal stress ratios were calculated along with the ratio between the maximum to the mean principal stress. The maximum dilatational energy density value will then represent a point in a corresponding curve (Fig. 2 a) of maximum dilatational energy density against applied strain.

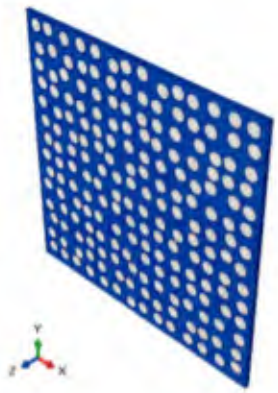

Fig. 1. 3-D RVE construction with total of 14x14 fibers.

For the three fiber volume fractions (40%, 54% and 60%), the maximum dilatational energy density is nearly constant with shear loading, and its value is relatively small compared to the distortional energy density. For example, in Fig. 3 (a), both the maximum dilatational and distortional energy densities are plotted for 40% fiber volume fraction and 100% nonuniformity. The dilatational energy density has a nearly constant value at all applied shear strains. This value is ~ 0.029 MPa, which is significantly lower than the critical value or brittle cavitation; meanwhile, the distortional energy density increases with applied shear strain. Also, for the same RVE, the condition of the equality of principal stress ratios for cavitation to occur is not fulfilled throughout the virtual test as shown in Fig. 2 (b). Similar Observations were found for the other fiber volume fractions and other degrees of nonuniformity. The threshold value of the distortional energy density for yielding reaches at a shear strain ~ 1.2%.

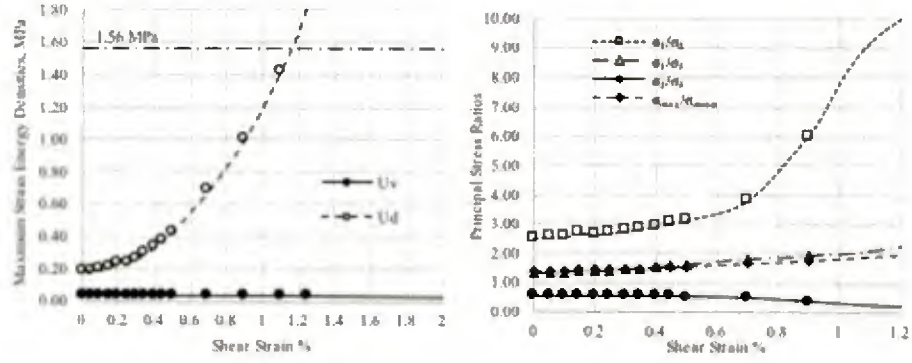

(a) (b)

Fig. 2. (a).The maximum values of dilatational energy density U_v and distortional energy density U_d attained within RVEs versus applied strain and (b) The principal stress ratios and the ratio of maximum/mean principal stress versus applied strain, for realization shown in Fig. 1 under axial shear loading.

For comparison, the results on the same RVE under transverse loading are sgown in Fig. 3 (a) and (b).

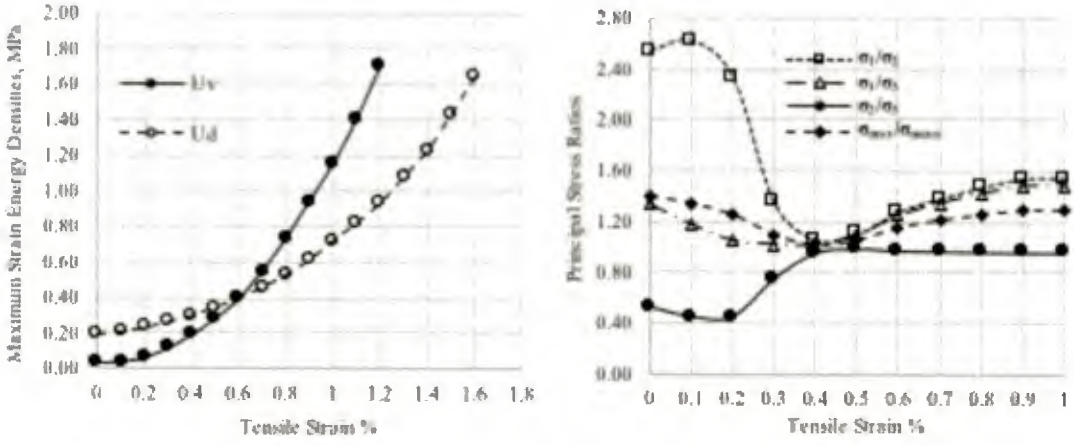

(a) (b)

Fig. 3. (a) The maximum values of dilatational energy density U_v and distortional energy density U_d attained within RVEs versus applied strain and (b) The principal stress ratios and the ratio of maximum/mean principal stress versus applied strain, for realization shown in Fig. 1 under transverse tensile loading.

The ongoing research will study combined loading consisting of axial shear and transverse tension.

Task 2.4 Periydnamic modeling of failure for the RVE studied with Synergistic Damage Mechanics

During this period we utilized the model developed at TAMU for an RVE of a fiber bundle in a composite loaded transversely. While the TAMU group used SDM to analyze the potential for cavitation, we (the UNL group) built a peridynamic model to study the failure initiation and propagation: from microcracks to macro-cracks under transverse quasi-staic loading conditions.

To accomplich this tasks we performed the following steps:

1. Reduction of problem size for Peridynamic (PD) computations: in order to reduce the size of the peridynamic model, we took the FEM model from TAMU (which included the embedded fiber bundle in a larger homogenized composite) and computed the displacements around the fiber bundle region to be applied onto the PD model (see Figure 4).

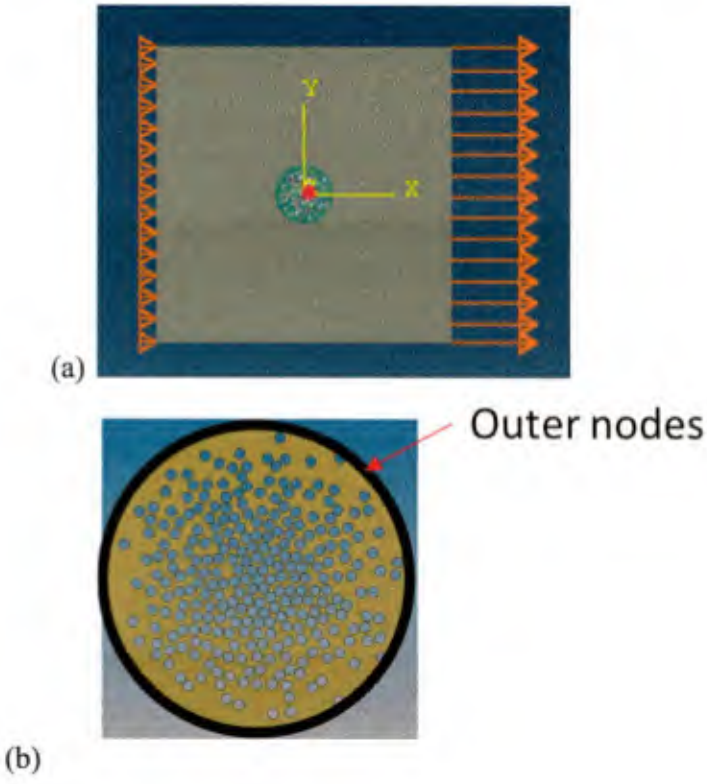

Fig. 4. (a) The geometry of the fiber bundle embedded in a homogenized composite and the loading conditions. (b) The detailed microstructure of the fiber bundle and the region where the displacement boundary conditions are applied in the PD model. Microstructure generated by the TAMU group.

2. Processing the PD model: to create the discretization for the PD model, we utilize a finite element grid; PD nodes are the centroids of finite elements, while areas of PD nodes are formed by the element areas of the finite elements; if the finite element mesh is nearly uniform (without sudden changes in node density), then the quadrature errors in the PD solution will be minimal; to replicate the material properties of the fibers and matrix phases in the PD model, we need to "disconnect" nodes that belong to two adjacent fibers, in case such nodes fall under the same horizon region; such bonds connecting nodes belonging to two different fibers need to be eliminated in the PD model since otherwise they would signify that different fibers are "glued" together by fiber material. Once this elimination process is performed, all nodal damage is reset to zero n the PD model, to represent the initially undamaged material.
3. We verified the reduced model by comparing the elastic deformations between an ABAQUS solution for the same reduced model and the PD model. The results (in terms of displacements along the direction of the applied load) are shown in Figure 5. The closesness between the finite element results and the PD results verify our implementation.
4. The evolution of failure in the PD model is shown in Figure 6. We notice the start of several microcracks from a number of different locations. These microcracks grow and eventually coalesce into a macrocrack. Such macro-cracks can lead to

full failure of the sample. Note that the applied boundary conditions are those from the FEM solution which did not include the failure process. Therefore, these boundary conditions are slightly different from the ones that take into account the failure process.

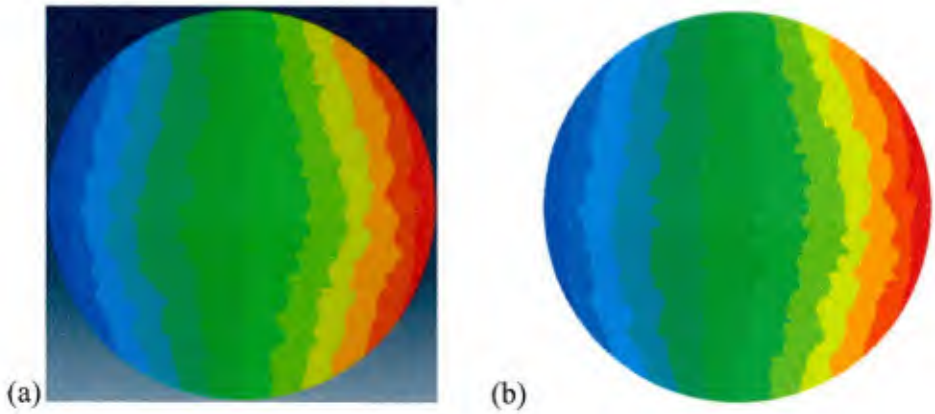

Fig. 5. Horizontal displacements for the fiber-bundle region: (a) results from a finite element solution with ABAQUS; (b) results from the PD model. Same color scheme was used in both cases.

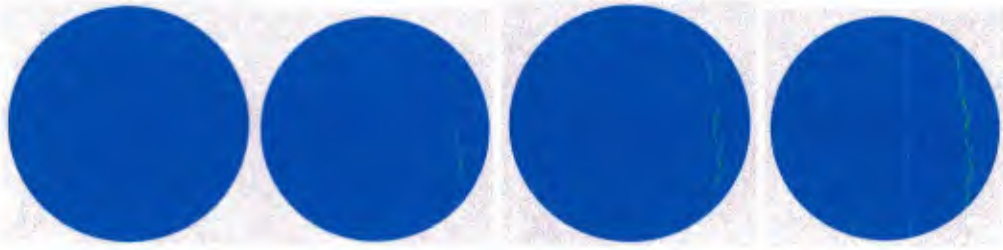

Fig. 6. Evolution of damage in the fiber-bundle region (see Fig. 4b): micro-crack initiation, coalescence, and appearance for a macro-crack.

The next steps are:

(a) We will study the failure behavior for different interface fracture values. This will allow us to understand thresholds between debonding and matrix cracks.

(b) We wil analyze the causes for differences seen between crack initiation and coalescence obtained by the PD approach and cavitation points obtained by the SDM approach.

(c) Employ an intermediate-homogenization approach to reduce the computational burden of explicit microstructure representations.